Published in IET Communications
Received on 9th December 2012
Revised on 27th March 2013
Accepted on 23rd April 2013
doi: 10.1049/iet-com.2013.0136

ISSN 1751-8628

Performance analysis of protograph low-density parity-check codes for Nakagami-*m* fading relay channels

Yi Fang[1,2], *Kai-Kit Wong*[2], *Lin Wang*[1], *Kin-Fai Tong*[2]

[1]*Department of Communication Engineering, Xiamen University, Xiamen, People's Republic of China*
[2]*Department of Electronic and Electrical Engineering, University College London, London, UK*
E-mail: wanglin@xmu.edu.cn

Abstract: In this study, the authors investigate the error performance of the protograph (low-density parity check) codes over Nakagami-*m* fading relay channels. The authors first calculate the decoding thresholds of the protograph codes over such channels with different fading depths (i.e. different values of *m*) by exploiting the modified protograph extrinsic information transfer (PEXIT) algorithm. Furthermore, based on the PEXIT analysis and using Gaussian approximation, the authors derive the bit-error-rate (BER) expressions for the error-free (EF) relaying protocol and decode-and-forward (DF) relaying protocol. The authors finally compare the threshold with the theoretical BER and the simulated BER results of the protograph codes. It reveals that the performance of DF protocol is approximately the same as that of EF protocol. Moreover, the theoretical BER expressions, which are shown to be reasonably consistent with the decoding thresholds and the simulated BERs, are able to evaluate the system performance and predict the decoding threshold with lower complexity as compared with the modified PEXIT algorithm. As a result, this work can facilitate the design of the protograph codes for the wireless communication systems.

1 Introduction

Spatial diversity is an effective technique to enhance the quality and reliability of wireless communications and can be typically achieved using multiple antennas at a transmitter and/or a receiver. Besides, spatial diversity can also be obtained by the use of relaying. The relay channel, which consists of a source, a relay and a destination, was probably first proposed in the 1970s [1]. Later, Cover and Gamal [2] have further developed the theory of such a channel. Recently, half-duplex relaying [3] has been verified to be relatively more practical in comparison with the full-duplex one because of simpler implementation.

To improve the performance, forward error correction codes have been applied to relay channels. As a capacity-approaching code, low-density parity-check (LDPC) code has been developed to significantly enhance the performance of relay channels for different channel conditions, such as non-fading [3–5] and fading scenarios [6, 7]. Moreover, Li *et al.* [8] provided the corresponding analysis of the LDPC-coded relay systems. At the same time, there has been a growing interest in protograph LDPC codes. It was shown in [9–11] that protograph (LDPC) codes not only achieve superior performance but also possess simple structures to realise linear encoding and decoding. For this reason, protograph codes have been used in additive white Gaussian noise (AWGN) relay channels [12], partial response channels [13] and Rayleigh-fading channels [14, 15]. However, so far, its analytical performance for general fading relay channels is not very well understood, which has motivated the results of this paper.

In this paper, we study the error performance of a half-duplex protograph LDPC-coded relay system over Nakagami-*m* fading channels. The Nakagami-*m* fading channel is a general type of fading channel that encompasses Rayleigh fading ($m = 1$) and AWGN ($m \to \infty$) channels as special cases. We first use the modified protograph extrinsic information transfer (PEXIT) algorithm [15] to analyse the decoding threshold of the protograph codes with different fading depths (i.e. different values of *m*). Afterwards, we derive the bit-error-rates (BERs) for the error-free (EF) and the decode-and-forward (DF) relaying protocols exploiting the modified PEXIT algorithm and using Gaussian approximation [16], and find that the BER analytical method has lower computational complexity than that of the modified PEXIT one. Simulated results show that the performance of the DF protocol approaches very close to that of EF, which align well with the analytical results. Furthermore, the results also indicate that the performance of the codes is improved as the fading depth decreases (higher *m*), but the rate of improvement is reduced simultaneously.

The remainder of this paper is organised as follows. In Section 2, the system model over the Nakagami-*m* fading channel is described. In Section 3, we analyse the protograph LDPC-coded relay system using the modified PEXIT algorithm. Moreover, we derive the BER

expressions of the protograph codes. Numerical results are carried out in Section 4, and conclusions are given in Section 5.

2 System model

We consider a two-hop half-duplex relay system model with one source, S, one relay, R, and one destination, D, as shown in Fig. 1. Each transmission period is divided into two time slots, with the first slot being the 'broadcast' time slot and the second slot being the 'cooperative' time slot. During the first time slot, S broadcasts the codeword to other terminals (including R and D). Then, in the second time slot, R cooperates with S to forward the re-encoded message of S–D whereas S remains idle. [In our model, we assume that the relay and the source adopt the same coding scheme.] During each transmission period, D stores the received codeword for decoding at the end of the second time slot. Mathematically, the received signals can be written as

$$r_{\mathrm{R1},j} = h_{\mathrm{SR},j}x_j + n_{\mathrm{SR},j} \tag{1}$$

$$r_{\mathrm{D1},j} = h_{\mathrm{SD},j}x_j + n_{\mathrm{SD},j} \tag{2}$$

$$r_{\mathrm{D2},j} = h_{\mathrm{RD},j}\hat{x}_j + n_{\mathrm{RD},j} \tag{3}$$

where, x_j and $\hat{x}_j$ denote the binary-phase-shift-keying (BPSK) modulated signals corresponding to the jth coded bit v_j and re-encoded bit $\hat{v}_j$, respectively; $r_{\mathrm{R1},j}$, $r_{\mathrm{D1},j}$ and $r_{\mathrm{D2},j}$ represent the received signals of the jth coded bit at the relay in the first time slot, at the destination in the first time slot and at the destination in the second time slot, respectively; $h_{\mathrm{SR},j}$, $h_{\mathrm{SD},j}$ and $h_{\mathrm{RD},j}$ are the mutually independent Nakagami-m fading channel coefficients of the S–R link, the S–D link and the R–D link, respectively; and $n_{\mathrm{SR},j}$, $n_{\mathrm{SD},j}$ and $n_{\mathrm{RD},j}$ are the AWGN with zero mean and variance of $\sigma_n^2\left(\sigma_n^2 = N_0 2\right)$.

We define the channel gain of the S–R link as $\gamma_{\mathrm{SR},j} = |h_{\mathrm{SR},j}|^2$ (similar expressions will be assumed for other links). Moreover, we assume that the receiver (R or D) knows perfectly the channel state information for decoding. At the destination, the signals from the source and relay are combined by a maximum ratio combiner (MRC). To simplify the analysis, we also assume that the distance from S to D is normalised to unity, whereas the distances from S to R and from R to D are d and $1-d$, respectively. [Note that the assumption of collinearity of S, R and D will not affect any of the derivation of our results.] Based on this assumption, we have $h_{\mathrm{SD},j} = \alpha_{\mathrm{SD},j}$, $h_{\mathrm{SR},j} = \alpha_{\mathrm{SR},j}/d$ and $h_{\mathrm{RD},j} = \alpha_{\mathrm{RD},j}/(1-d)$, where α is the Nakagami-m fading parameter with the probability density function expressed as

$$f(x) = \frac{2}{\Gamma(m)}\left(\frac{m}{\Omega}\right)^m x^{2m-1}\exp\left(-\frac{m}{\Omega}x^2\right), \quad \text{for } m \geq 0.5 \tag{4}$$

where m is the fading depth, $\Omega = \mathbb{E}\left[\alpha^2\right] = 1$, $\mathbb{E}[\cdot]$ is the expectation operator and $\Gamma(\cdot)$ is the Gamma function. In this paper, we focus on ergodic channels, in which the channel fades significantly rapidly such that it varies bit by bit. [Although we consider the ergodic (i.e. fast fading) scenario here, the results in this paper are also applicable for the quasi-static case (where the fading parameter of each link is kept to be constant for a code block).]

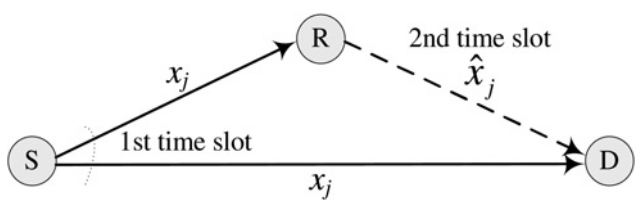

Fig. 1 *System model of the protograph LDPC-coded relay system over fading channels*

3 Performance analysis

In this section, we derive the BER expression of the protograph code in our system with the EF and DF protocols based on the modified PEXIT algorithm and using Gaussian approximation [16]. In the analysis, it is assumed that the all-zero codeword is transmitted and the block length of the code is infinite [17]. The output (extrinsic and a posteriori) log-likelihood-ratio (LLR) messages of Nakagami-m fading channels are approximately following the symmetric Gaussian distribution [18].

Firstly, we review the protograph code [9]. A protograph is a Tanner graph with a relatively small number of nodes. A protograph code is a large protograph (called derived graph) obtained by the 'copy-and-permute' operation on a protograph. Accordingly, a code with different block lengths can be produced by different number of times of the 'copy-and-permute' operation. A protograph with N variable nodes and M check nodes can be described by a base matrix $\boldsymbol{B} = (b_{i,j})$ with dimensions $M \times N$, where $b_{i,j}$ denotes the number of edges connecting the variable node v_j to the check node c_i. Since the protograph code always has some punctured variable nodes, we define P_j as the punctured label of v_j ($P_j = 0$ if v_j is punctured; otherwise $P_j = 1$). We also define the following LLRs and mutual information (MI).

LLR value:

- $L_{\mathrm{Av}}(i, j)$ denotes the input (a priori) LLR value of v_j corresponding to c_i on each of the $b_{i,j}$ edges.
- $L_{\mathrm{Ac}}(i, j)$ denotes the input (a priori) LLR value of c_i corresponding to v_j on each of the $b_{i,j}$ edges.
- $L_{\mathrm{Ev}}(i, j)$ denotes the output (extrinsic) LLR value passing from v_j to the c_i.
- $L_{\mathrm{Ec}}(i, j)$ denotes the output (extrinsic) LLR value passing from c_i to the v_j.
- $L_{\mathrm{app}}(j)$ denotes the a-posteriori LLR value of v_j.

MI:

- $I_{\mathrm{Av}}(i, j)$ denotes the a-priori MI between $L_{\mathrm{Av}}(i, j)$ and the corresponding coded bit v_j.
- $I_{\mathrm{Ac}}(i, j)$ denotes the a-priori MI between $L_{\mathrm{Ac}}(i, j)$ and the corresponding coded bit v_j.
- $I_{\mathrm{Ev}}(i, j)$ denotes the extrinsic MI between $L_{\mathrm{Ev}}(i, j)$ and the corresponding coded bit v_j.
- $I_{\mathrm{Ec}}(i, j)$ denotes the extrinsic MI between $L_{\mathrm{Ec}}(i, j)$ and the corresponding coded bit v_j.

doi: 10.1049/iet-com.2013.0136

• $I_{app}(j)$ denotes the a-posteriori MI between $L_{app}(j)$ and the corresponding coded bit v_j.

Note that the subscripts 'SR', 'SD', 'RD' and 'D' are used to denote the S–R link, the S–D link, the R–D link and the destination, respectively. For example, $L_{SR-Av}(i, j)$ represents the a-priori LLR value of v_j corresponding to c_i on each of the $b_{i,j}$ edges of the S–R link.

3.1 BER of EF relaying protocol

At the destination receiver, the output of MRC corresponding to the jth coded bit is given by

$$y_{D,j} = h_{SD,j} r_{D1,j} + h_{RD,j} r_{D2,j} \tag{5}$$

Afterwards, the initial LLR value $L_{D-ch,j}$ of the jth coded bit is calculated as (see (6))

where $\Pr(\cdot)$ denotes the probability function, $\boldsymbol{h}_j = \{h_{SR,j}, h_{SD,j}, h_{RD,j}\}$ is the channel vector, $\gamma_{SD,j} = |h_{SD,j}|^2 = \alpha_{SD,j}^2$, $\gamma_{RD,j} = |h_{RD,j}|^2 = \alpha_{RD,j}^2/(1-d)^2$ and $x_j = \hat{x}_j$ (EF decoding at the relay).

Based on the all-zero codeword assumption ($x_j = +1$), given a fixed channel realisation (a fixed fading vector $\boldsymbol{h}_j$), we can easily obtain the expectation and the variance of $L_{D-ch,j}$, resulting in

$$\mathbb{E}\left[L_{D-ch,j}\right] = \frac{2}{\sigma_n^2}\left(\gamma_{SD,j} + \gamma_{RD,j}\right) = \frac{2}{\sigma_n^2}\lambda_{D,j} \tag{7}$$

$$\mathrm{var}\left[L_{D-ch,j}\right] = \frac{4}{\sigma_n^4}\left(\gamma_{SD,j}\sigma_n^2 + \gamma_{RD,j}\sigma_n^2\right) = \frac{4}{\sigma_n^2}\lambda_{D,j} \tag{8}$$

where $\lambda_{D,j}$ is the short-hand notation of $\gamma_{SD,j} + \gamma_{RD,j}$. As seen from (7) and (8), $L_{D-ch,j}$ follows the symmetric Gaussian distribution, that is, $L_{D-ch,j} \sim \mathcal{N}\left(\left(2/\left(\sigma_n^2\right)\right)\lambda_{D,j}, \left(4/\left(\sigma_n^2\right)\right)\lambda_{D,j}\right)$. Subsequently, substituting $\sigma_n^2 = \left(1/\left(2R\left(E_{b'}/N_0\right)\right)\right)$ into (8) [$E_{b'} = ((E_b)/2)$, the normalised factor 1/2 is used to keep the total energy per transmitted symbol to be E_s] and considering the punctured label P_j, we have

$$\mathrm{var}\left[L_{D-ch,j}\right] = 8RP_j\lambda_{D,j}\left(E_{b'}/N_0\right) = 4RP_j\lambda_{D,j}\left(E_b/N_0\right) \tag{9}$$

Thus, the modified PEXIT algorithm [15] can be applied to our system by using the expression (9). [According to Fang *et al.* [15], the maximum iteration number of the modified PEXIT algorithm T_{max}^{P} should be large enough in order to ensure the complete convergence of the decoder, that is, $T_{max}^{P} \geq 500$.]

For the qth ($q = 1, 2, \ldots, Q$, where Q is the total number of channel realisations [To ensure the accuracy of our derived BER expressions, Q should be set to a sufficiently large integer, that is, $Q \geq 10^5$.]) channel realisation $h_{q,j}$, the a-posteriori LLR of v_j during the $(t+1)$th iteration is written as

$$L_{D-app,q}^{t+1}(j) = \sum_{i=1}^{M} b_{i,j} L_{D-Av,q}^{t+1}(i, j) + L_{D-ch,q,j} \tag{10}$$

The expected value of $L_{D-Av,q}^{t+1}(i, j)$ is then expressed by

$$\bar{L}_{D-app}^{t+1}(j) = \mathbb{E}\left[L_{D-app,q}^{t+1}(j)\right] = \frac{1}{Q}\sum_{q=1}^{Q} L_{D-app,q}^{t+1}(j) \tag{11}$$

As the output LLR values, that is, the extrinsic LLR and a-posteriori LLR, are approximated to follow a symmetric Gaussian distribution, we can evaluate the variance of $\bar{L}_{D-app}^{t+1}(j)$ as

$$\begin{aligned}\mathrm{var}\left[\bar{L}_{D-app}^{t+1}(j)\right] &= \left\{J^{-1}\left(\bar{I}_{D-app}^{t+1}(j)\right)\right\}^2 \\ &= \left\{J^{-1}\left(\mathbb{E}\left[I_{D-app,q}^{t+1}(j)\right]\right)\right\}^2\end{aligned} \tag{12}$$

where

$$\bar{I}_{D-app}^{t+1}(j) = \mathbb{E}\left[I_{D-app,q}^{t+1}(j)\right] = (1/Q)\sum_{q=1}^{Q} I_{D-app,q}^{t+1}(j)$$

is the expected value of $I_{D-app,q}^{t+1}(j)$ over all channel realisations, the expression of the a-posteriori MI $I_{D-app,q}^{t+1}(j)$ is obtained as [15, (21)], denoted by $I_{D-app,q}^{t+1}(j) = F\left(I_{D-Av,q}^{t+1}(1, j), \ldots, I_{D-Av,q}^{t+1}(M, j); \mathrm{var}\left[L_{D-ch,q,j}\right]\right)$ and $J(\sigma_{ch})$ is the MI between a BPSK modulated bit and its LLR value $L_{ch} \sim \mathcal{N}\left(\left(\left(\sigma_{ch}^2\right)/2\right), \sigma_{ch}^2\right)$ over an AWGN

$$\begin{aligned}L_{D-ch,j} &= \ln\frac{\Pr\left(v_j = 0 | y_{D,j}, \boldsymbol{h}_j\right)}{\Pr\left(v_j = 1 | y_{D,j}, \boldsymbol{h}_j\right)} = \ln\frac{\Pr\left(x_j = +1 | y_{D,j}, \boldsymbol{h}_j\right)}{\Pr\left(x_j = -1 | y_{D,j}, \boldsymbol{h}_j\right)} \\ &= \frac{2y_{D,j}}{\sigma_n^2} = \frac{2}{\sigma_n^2}\left(h_{SD,j} r_{D1,j} + h_{RD,j} r_{D2,j}\right) \\ &= \frac{2}{\sigma_n^2}\left[h_{SD,j}\left(h_{SD,j}x_j + n_{SD,j}\right) + h_{RD,j}\left(h_{RD,j}\hat{x}_j + n_{RD,j}\right)\right] \\ &= \frac{2}{\sigma_n^2}\left[|h_{SD,j}|^2 x_j + |h_{RD,j}|^2\hat{x}_j + h_{SD,j}n_{SD,j} + h_{RD,j}n_{RD,j}\right] \\ &= \frac{2}{\sigma_n^2}\left[\left(\gamma_{SD,j} + \gamma_{RD,j}\right)x_j + h_{SD,j}n_{SD,j} + h_{RD,j}n_{RD,j}\right]\end{aligned} \tag{6}$$

channel, represented as [17]

$$J(\sigma_{\text{ch}}) = 1 - \int_{-\infty}^{\infty} \frac{\exp\left(-\left(\left((\xi - \sigma_{\text{ch}}^2/2)^2\right)/(2\sigma_{\text{ch}}^2)\right)\right)}{\sqrt{2\pi\sigma_{\text{ch}}^2}} \times \log_2\left[1 + \exp(-\xi)\right] \mathrm{d}\xi \quad (13)$$

The corresponding inverse function is given by [17]

$$J^{-1}(x) = \begin{cases} \eta_1 x^2 + \eta_2 x + \eta_3\sqrt{x}, & \text{if } 0 \le x \le 0.3646 \\ \eta_4 \ln\left[\eta_5(1-x)\right] + \eta_6 x, & \text{otherwise} \end{cases} \quad (14)$$

where $\eta_1 = 1.09542$, $\eta_2 = 0.214217$, $\eta_3 = 2.33737$, $\eta_4 = -0.706692$, $\eta_5 = 0.386013$ and $\eta_6 = 1.75017$. With the help of (12)–(14), the BER of the jth variable node after t iterations is evaluated by

$$\begin{aligned} P_{\text{D}-b}^{t+1}(j) &= \frac{1}{2}\Pr\left(\bar{L}_{\text{D}-\text{app}}^{t+1}(j) < 0 | x_j = +1\right) \\ &\quad + \frac{1}{2}\Pr\left(\bar{L}_{\text{D}-\text{app}}^{t+1}(j) \ge 0 | x_j = -1\right) \\ &= \frac{1}{2}\text{erfc}\left(\frac{\mathbb{E}\left[\bar{L}_{\text{D}-\text{app}}^{t+1}(j) | x_j = +1\right]}{\sqrt{2\text{var}\left[\bar{L}_{\text{D}-\text{app}}^{t+1}(j) | x_j = +1\right]}}\right) \\ &= \frac{1}{2}\text{erfc}\left(\frac{\text{var}\left[\bar{L}_{\text{D}-\text{app}}^{t+1}(j) | x_j = +1\right]/2}{\sqrt{2\text{var}\left[\bar{L}_{\text{D}-\text{app}}^{t+1}(j) | x_j = +1\right]}}\right) \\ &= \frac{1}{2}\text{erfc}\left(\frac{\sqrt{\text{var}\left[\bar{L}_{\text{D}-\text{app}}^{t+1}(j) | x_j = +1\right]}}{2\sqrt{2}}\right) \\ &= \frac{1}{2}\text{erfc}\left(\frac{J^{-1}\left(\bar{I}_{\text{D}-\text{app}}^{t+1}(j)\right)}{2\sqrt{2}}\right) \end{aligned} \quad (15)$$

where erfc(·) is the complementary error function, defined as $\text{erfc}(x) = \left(2/\left(\sqrt{\pi}\right)\right)\int_x^{\infty} \text{e}^{-\tau^2}\,\mathrm{d}\tau$.

Finally, the averaged BER of a protograph code after t iterations is written as

$$\begin{aligned} P_{\text{EF}-b}^{t+1} &= P_{\text{D}-b}^{t+1} = \frac{1}{N}\sum_{j=1}^{N} P_{\text{D}-b}^{t+1}(j) \\ &= \frac{1}{2N}\sum_{j=1}^{N} \text{erfc}\left(\frac{J^{-1}\left(\bar{I}_{\text{D}-\text{app}}^{t+1}(j)\right)}{2\sqrt{2}}\right) \end{aligned} \quad (16)$$

3.2 BER of DF relaying protocol

In DF, if the relay can decode received signals correctly, it re-encodes the decoded information and then forwards them to the destination; otherwise, it does not send message or remains idle. Consequently, the BER of the DF protocol of the jth variable node after t iterations can be found as

$$P_{\text{DF}-b}^{t+1}(j) = P_{\text{SR}-b}^{t+1}(j)P_{\text{SD}-b}^{t+1}(j) + \left[1 - P_{\text{SR}-b}^{t+1}(j)\right]P_{\text{D}-b}^{t+1}(j) \quad (17)$$

where $P_{\text{SR}-b}^{t+1}(j)$, $P_{\text{SD}-b}^{t+1}(j)$ and $P_{\text{D}-b}^{t+1}(j)$ are the corresponding BERs of the jth variable node after t iterations at the relay receiver with the signal from source, at the destination receiver with one signal from the source and at the destination receiver with two signals both from the source and relay (i.e. BER of the EF protocol), respectively.

The initial LLR of the jth variable node of the S–R link is expressed by [18]

$$\begin{aligned} L_{\text{SR}-\text{ch},\,j} &= \frac{2h_{\text{SR},\,j}r_{\text{R1},\,j}}{\sigma_n^2} = \frac{2h_{\text{SR},\,j}}{\sigma_n^2}\left(h_{\text{SR},\,j}x_j + n_{\text{SR},\,j}\right) \\ &= \frac{2}{\sigma_n^2}\left(\gamma_{\text{SR},\,j}x_j + h_{\text{SR},\,j}n_{\text{SR},\,j}\right) \end{aligned} \quad (18)$$

In (18), we have $\mathbb{E}\left[L_{\text{SR}-\text{ch},\,j}\right] = \left(\left(2\gamma_{\text{SR},\,j}\right)/\left(\sigma_n^2\right)\right)$ and $\text{var}\left[L_{\text{SR}-\text{ch},\,j}\right] = \left(\left(4\gamma_{\text{SR},\,j}\right)/\left(\sigma_n^2\right)\right)$. Hence, during the $(t+1)$th iteration, the a-posteriori MI of the jth variable for the qth ($q = 1, 2, \ldots, Q$) channel realisation and the corresponding expected value are, respectively, given by

$$I_{\text{SR}-\text{app},\,q}^{t+1}(j) = F\left(I_{\text{SR}-\text{Av},\,q}^{t+1}(1,\,j),\,\ldots,\,I_{\text{SR}-\text{Av},\,q}^{t+1}(M,\,j);\,\text{var}\left[L_{\text{SR}-\text{ch},\,q,\,j}\right]\right) \quad (19)$$

$$\bar{I}_{\text{SR}-\text{app}}^{t+1}(j) = \mathbb{E}\left[I_{\text{SR}-\text{app},\,q}^{t+1}(j)\right] = \frac{1}{Q}\sum_{q=1}^{Q} I_{\text{SR}-\text{app},\,q}^{t+1}(j) \quad (20)$$

Further, the variance of the expected a-posteriori LLR associated with (20) is yielded in terms of the Gaussian assumption

$$\text{var}\left[\bar{L}_{\text{SR}-\text{app}}^{t+1}(j)\right] = \left\{J^{-1}\left(\bar{I}_{\text{SR}-\text{app}}^{t+1}(j)\right)\right\}^2 \quad (21)$$

Note that

$$\mathbb{E}\left[\bar{L}_{\text{SR}-\text{app}}^{t+1}(j)\right] = \text{var}\left[\bar{L}_{\text{SR}-\text{app}}^{t+1}(j)\right]/2$$

Using (21), we can therefore obtain the BER of the jth variable after t iterations as

$$\begin{aligned} P_{\text{SR}-b}^{t+1}(j) &= \frac{1}{2}\text{erfc}\left(\frac{\mathbb{E}\left[\bar{L}_{\text{SR}-\text{app}}^{t+1}(j) | x_j = +1\right]}{\sqrt{2\text{var}\left[\bar{L}_{\text{SR}-\text{app}}^{t+1}(j) | x_j = +1\right]}}\right) \\ &= \frac{1}{2}\text{erfc}\left(\frac{J^{-1}\left(\bar{I}_{\text{SR}-\text{app}}^{t+1}(j)\right)}{2\sqrt{2}}\right) \end{aligned} \quad (22)$$

Likewise, the BER of the jth variable after t iterations of the

doi: 10.1049/iet-com.2013.0136

S–D link can be written as

$$P_{\mathrm{SD}-b}^{t+1}(j)=\frac{1}{2}\mathrm{erfc}\left(\frac{J^{-1}\left(\bar{I}_{\mathrm{SD-app}}^{t+1}(j)\right)}{2\sqrt{2}}\right) \tag{23}$$

with the parameters subjected to (see (24))
where $L_{\mathrm{SD-ch},\,q,\,j}$ is the initial LLR of v_j for the qth S–D link realisation and $\gamma_{\mathrm{SD},\,q,\,j}=|h_{\mathrm{SD},\,q,\,j}|^2$.

Substituting (15), (22) and (23) into (17), the BER of the jth variable node with DF after t iterations can be formulated. Finally, we obtain the averaged BER with DF protocol after t iterations as

$$P_{\mathrm{DF}-b}^{t+1}=\frac{1}{N}\sum_{j=1}^{N}P_{\mathrm{DF}-b}^{t+1}(j) \tag{25}$$

Note also that

- The maximum number of iterations of the theoretical BER analysis $T_{\max}$ ($t=T_{\max}$) equals to that of the simulations ($T_{\max}$ is always much smaller than $T_{\max}^{\mathrm{P}}$). In this paper, we set $T_{\max}=100$ as in [15, 19]. Therefore its computational complexity can be reduced by $\left(T_{\max}^{\mathrm{P}}-T_{\max}\right)/T_{\max}^{\mathrm{P}}$ as compared with the modified PEXIT algorithm.
- The BER analysis can be used to evaluate the performance of the protograph codes for any E_b/N_0 and $T_{\max}$, whereas the modified PEXIT algorithm can only be exploited to derive the E_b/N_0 threshold above which an arbitrarily small BER can be achieved (i.e. all the code blocks can be successfully decoded) for a sufficiently large $T_{\max}^{\mathrm{P}}$.

4 Numerical results and discussions

In this section, we firstly analyse the decoding threshold of two typical protograph codes, that is, the AR3A and AR4JA codes, over Nakagami-m fading relay channels utilising the modified PEXIT algorithm [15]. Then, we compare the decoding thresholds, the theoretical BER and simulated BER results of the two protograph codes. For all the following results, the distance of S–R link d is set to 0.4.

The AR3A and AR4JA codes, which have been proposed by Jet Propulsion Laboratory [10, 11], can, respectively, accomplish excellent performance in the low SNR region and the high SNR region over the AWGN channel. The corresponding base matrices of these two codes with a code rate of $R=((n+1)/(n+2))$, denoted by $\boldsymbol{B}_{A3}$ and $\boldsymbol{B}_{A4}$, respectively, are given by

$$\boldsymbol{B}_{A3}=\begin{pmatrix}1 & 2 & 1 & 0 & \overbrace{0\,0\,\cdots\,0\,0}^{2n}\\ 2 & 1 & 1 & 1 & 2\,1\,\cdots\,2\,1\\ 2 & 1 & 1 & 1 & 1\,2\,\cdots\,1\,2\end{pmatrix} \tag{26}$$

$$\boldsymbol{B}_{A4}=\begin{pmatrix}1 & 2 & 0 & 0 & 0 & \overbrace{0\,0\,\cdots\,0\,0}^{2n}\\ 0 & 3 & 1 & 1 & 1 & 3\,1\,\cdots\,3\,1\\ 0 & 1 & 2 & 2 & 1 & 1\,3\,\cdots\,1\,3\end{pmatrix} \tag{27}$$

In (26) and (27), the jth column corresponds to the jth variable node and the ith row refers to the ith check node. The variable nodes corresponding to the second columns of the two matrices are punctured.

4.1 Decoding threshold analysis

We calculate the decoding thresholds of the AR3A and AR4JA codes with different code rates and different fading depths using the modified PEXIT algorithm [15] and show the result in Table 1. [For the threshold analysis, we only consider the perfect S–R channel (i.e. EF), as is typical in many practical cases [20].] As seen from this table, the threshold of the AR3A code is lower than that of the AR4JA code for a fixed code rate and fading depth (fixed R and m). For instance, the thresholds of the AR3A code and the AR4JA code are 0.575 and 0.722 dB, respectively, with parameters $R=4/5$ and $m=2$. Moreover, the threshold is reduced as the fading depth decreases (higher m) for both the two codes and hence the error performance should be improved in the waterfall region. However, the decrease of the threshold is reduced when m becomes larger, indicating that the rate of performance improvement is reduced.

Table 1 Decoding thresholds $(E_b/N_0)_{\mathrm{th}}$ (dB) of the AR3A code and AR4JA code with different code rates over Nakagami-fading relay channels with different fading depths $m=1$, 2, 3 and 4.

Code rate	AR3A code				AR4JA code			
	$m=1$	$m=2$	$m=3$	$m=4$	$m=1$	$m=2$	$m=3$	$m=4$
1/2($n=0$)	− 1.345	− 1.825	− 1.983	− 2.056	− 1.187	− 1.675	− 1.828	− 1.895
2/3($n=1$)	0.004	− 0.759	− 0.994	− 1.098	0.162	− 0.566	− 0.823	− 0.918
3/4($n=2$)	0.890	− 0.016	− 0.316	− 0.472	1.128	0.185	− 0.136	− 0.292
4/5($n=3$)	1.639	0.575	0.216	0.037	1.805	0.722	0.382	0.192
5/6($n=4$)	2.235	1.042	0.653	0.454	2.392	1.164	0.785	0.576
6/7($n=5$)	2.732	1.404	0.991	0.778	2.855	1.533	1.092	0.887
7/8($n=6$)	3.158	1.748	1.278	1.044	3.284	1.852	1.379	1.150

$$\begin{cases}\bar{I}_{\mathrm{SD-app}}^{t+1}(j)=\mathbb{E}\left[I_{\mathrm{SD-app},\,q}^{t+1}(j)\right]=\dfrac{1}{Q}\displaystyle\sum_{q=1}^{Q}I_{\mathrm{SD-app},\,q}^{t+1}(j)\\ I_{\mathrm{SD-app},\,q}^{t+1}(j)=F\left(I_{\mathrm{SD-Av},\,q}^{t+1}(1,\,j),\,\ldots,I_{\mathrm{SD-Av},\,q}^{t+1}(M,\,j);\,\mathrm{var}\left[L_{\mathrm{SD-ch},\,q,\,j}\right]\right)\\ \mathrm{var}\left[L_{\mathrm{SD-ch},\,q,\,j}\right]=\dfrac{4\gamma_{\mathrm{SD},\,q,\,j}}{\sigma_n^2}\end{cases} \tag{24}$$

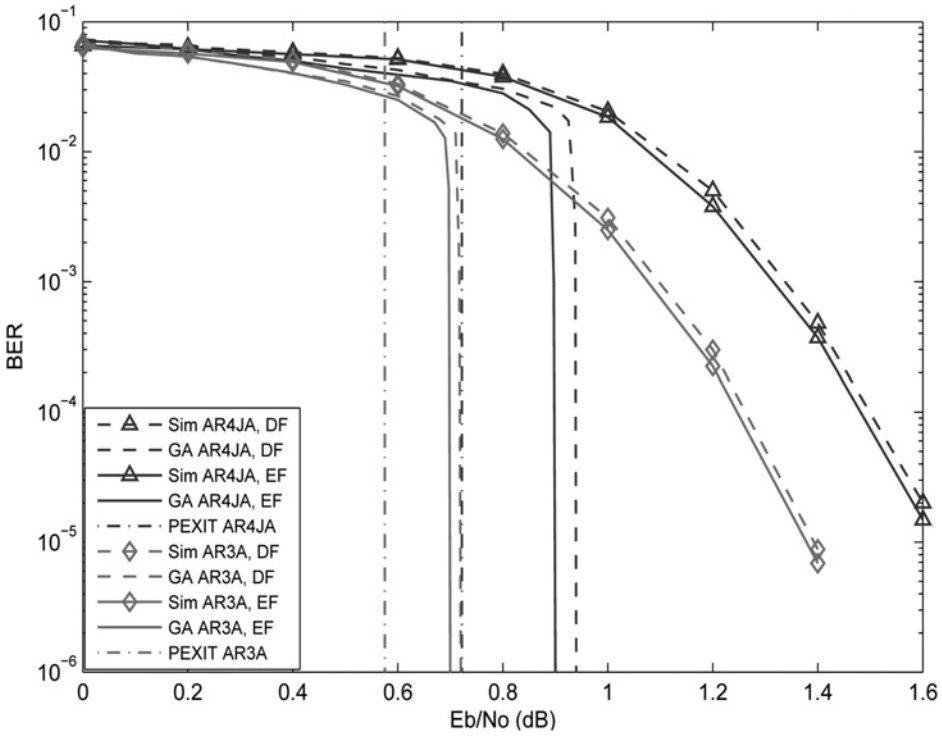

Fig. 2 *BER results of AR3A and AR4JA codes over Nakagami-fading relay channels with the fading depth m = 2*

4.2 BER performance

In the sequel, we present the simulated results of the AR3A and AR4JA codes with a code rate of $R = 4/5$ and compare their simulated and theoretical BER curves with the decoding thresholds. We denote N_p, K_p and L_p as the block length, the information length and the punctured length of the code, respectively. Unless specified otherwise, in the simulations, it has been assumed that the decoder performs a maximum of 100 iterations for each code block with parameters $[N_p, K_p, L_p] = [5632, 4096, 512]$.

In Fig. 2, we show the BER results (against E_b/N_0) of the AR4JA and AR3A codes over Nakagami-fading relay channels with DF and EF protocols. The fading depth m is set to 2. As seen, the error performance of the codes with the DF protocol approaches closely to that with EF, which suggests that the relay can decode most of the received

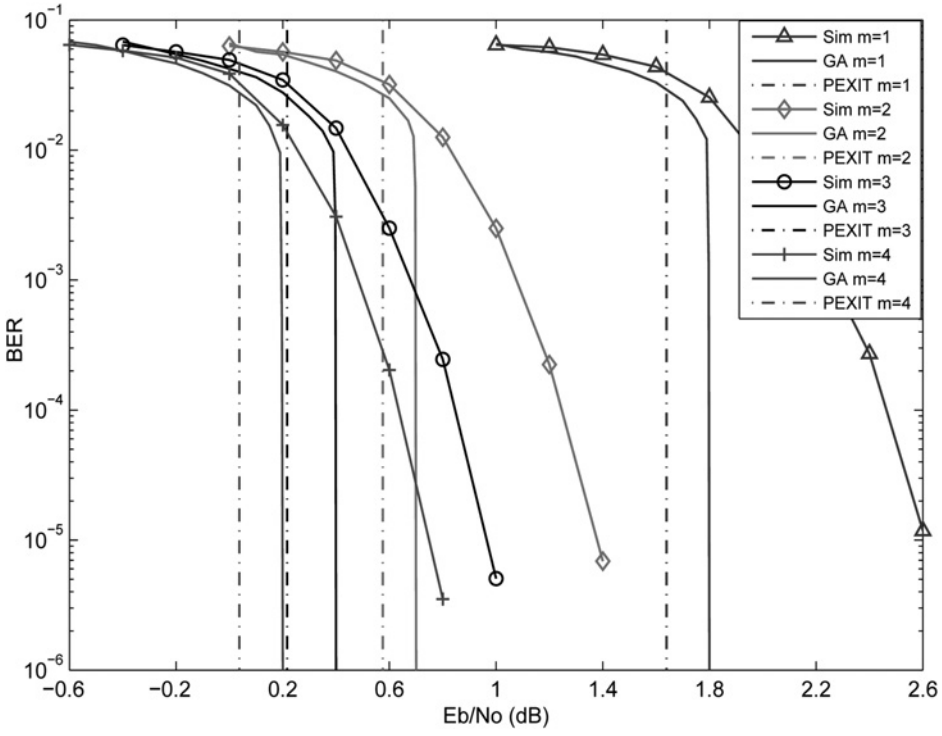

Fig. 3 *BER results of the AR3A code over Nakagami-fading relay channels with different fading depths (m = 1, 2, 3 and 4)*

doi: 10.1049/iet-com.2013.0136

code blocks successfully. Moreover, the AR3A code outperforms the AR4JA codes for the range of E_b/N_0 under study. At a BER of 10^{-5}, the AR3A code achieves a gain ~ 0.2 dB as compared with the AR4JA code both for the DF and EF protocols. In the same figure, consider the AR3A code with DF protocol at a BER of 10^{-5}, the theoretical BER result is in good agreement with the PEXIT threshold within 0.2 dB. Moreover, the corresponding simulated curve has another gap about 0.7 dB to the theoretical one, which is reasonably consistent with the results in [16, 19]. It is because our theoretical BER formulas are derived subjecting to the infinite-block length assumption.

Fig. 3 presents the BER results (against E_b/N_0) of the AR3A code in the EF relay systems for different fading depths ($m = 1$, 2, 3 and 4). As E_b/N_0 increases steadily, both the two codes start to perform better for a larger value of m in terms of the thresholds, the theoretical and simulated BER curves. Nevertheless, the improved gain is reduced as m increases. For example, at a BER of 10^{-5}, the improved gains are about 1.2, 0.45 and 0.25 dB as m increases from 1 to 2, 2 to 3 and 3 to 4, respectively. Moreover, it can be observed that the gaps between the theoretical BERs and the simulated results are around 0.8, 0.7, 0.55 and 0.5 dB for $m = 1$, 2, 3 and 4, respectively. Simulations have also been performed for the AR4JA code and with the DF protocol, and similar observations are obtained.

5 Conclusions

The performance of the protograph LDPC codes over Nakagami-m fading relay channels has been studied. The BER expressions for the protograph codes with DF and EF relaying protocols have been derived using the modified PEXIT algorithm and Gaussian approximation. The decoding threshold, the theoretical BER and the simulated BER results have shown that the error performance of the DF protocol is very close to that of EF, which suggests that the relay can decode most received codewords correctly. The differences between the threshold and the theoretical BER and between the theoretical BER and the simulated BER have been found to be about 0.15–0.2 and 0.5–0.8 dB, respectively, showing a reasonable consistence. Consequently, our analytical expressions not only can provide a good approximation of the system performance for a large-block length but also predict accurately the decoding threshold more efficiently in comparison with the modified PEXIT algorithm.

6 Acknowledgments

The authors thank the anonymous reviewers for their valuable comments that have helped improving the overall quality of the paper. This work was partially supported by the NSF of China (nos. 61271241, 61001073 and 61102134), the European Union-FP7 (CoNHealth, no. 294923) as well as the Fundamental Research Funds for the Central Universities (No. 201112G017).

7 References

1 van der Meulen, E.C.: 'Three-terminal communication channels', *Adv. Appl. Probab.*, 1971, **3**, pp. 120–154
2 Cover, T., Gamal, A.: 'Capacity theorems for the relay channel', *IEEE Trans. Inf. Theory*, 1979, **25**, (5), pp. 572–584
3 Chakrabarti, A., de Baynast, A., Sabharwal, A., Aazhang, B.: 'Low density parity check codes for the relay channel', *IEEE J. Sel. Areas Commun.*, 2007, **25**, (2), pp. 280–291
4 Razaghi, P., Yu, W.: 'Bilayer low-density parity-check codes for decode-and-forward in relay channels', *IEEE Trans. Inf. Theory*, 2007, **53**, (10), pp. 3723–3739
5 Li, C., Yue, G., Wang, X., Khojastepour, M.: 'LDPC code design for half-duplex cooperative relay', *IEEE Trans. Wirel. Commun.*, 2008, **7**, (11), pp. 4558–4567
6 Hu, J., Duman, T.: 'Low density parity check codes over half-duplex relay channels'. Proc. 2006 IEEE Int. Symp. Information Theory (ISIT'06), July 2006, pp. 972–976
7 Vahabzadeh, O., Salehi, M.: 'Design of bilayer lengthened LDPC codes for Rayleigh fading relay channels'. Proc. 2011 Annual Conf. Information Sciences and Systems (CISS), March 2011, pp. 1–5
8 Li, C., Yue, G., Khojastepour, M., Wang, X., Madihian, M.: 'LDPC-coded cooperative relay systems: performance analysis and code design', *IEEE Trans. Commun.*, 2008, **56**, (3), pp. 485–496
9 Thorpe, J.: 'Low-density parity-check (LDPC) codes constructed from protographs'. Proc. IPN Progress Report, 2003, pp. 42–154
10 Abbasfar, A., Divsalar, D., Yao, K.: 'Accumulate-repeat-accumulate codes', *IEEE Trans. Commun.*, 2007, **55**, (4), pp. 692–702
11 Divsalar, D., Dolinar, S., Jones, C., Andrews, K.: 'Capacity-approaching protograph codes', *IEEE J. Sel. Areas Commun.*, 2009, **27**, (6), pp. 876–888
12 Nguyen, T.V., Nosratinia, A., Divsalar, D.: 'Bilayer protograph codes for half-duplex relay channels'. Proc. 2010 IEEE Int. Symp. Information Theory (ISIT'10), June 2010, pp. 948–952
13 Fang, Y., Chen, P., Wang, L., Lau, F.C.M.: 'Design of protograph LDPC codes for partial response channels', *IEEE Trans. Commun.*, 2012, **60**, (10), pp. 2809–2819
14 Nguyen, T.V., Nosratinia, A., Divsalar, D.: 'Threshold of protograph-based LDPC coded BICM for Rayleigh fading'. Proc. IEEE Global Telecommunication Conf., December 2011, pp. 1–5
15 Fang, Y., Chen, P., Wang, L., Lau, F.C.M., Wong, K.K.: 'Performance analysis of protograph-based LDPC codes with spatial diversity', *IET Commun.*, 2012, **6**, (17), pp. 2941–2948
16 Lehmann, F., Maggio, G.: 'Analysis of the iterative decoding of LDPC and product codes using the Gaussian approximation', *IEEE Trans. Inf. Theory*, 2003, **49**, (11), pp. 2993–3000
17 ten Brink, S., Kramer, G., Ashikhmin, A.: 'Design of low-density parity-check codes for modulation and detection', *IEEE Trans. Commun.*, 2004, **52**, (4), pp. 670–678
18 Hou, J., Siegel, P., Milstein, L.: 'Performance analysis and code optimization of low density parity-check codes on Rayleigh fading channels', *IEEE J. Sel. Areas Commun.*, 2001, **19**, (5), pp. 924–934
19 Tan, B.S., Li, K.H., Teh, K.C.: 'Performance analysis of LDPC codes with maximum-ratio combining cascaded with selection combining over Nakagami-m fading', *IEEE Trans. Wirel. Commun.*, 2011, **10**, (6), pp. 1886–1894
20 Duyck, D., Capirone, D., Boutros, J.J., Moeneclaey, M.: 'Analysis and construction of full-diversity joint network-LDPC codes for cooperative communications', *EURASIP J. Wirel. Commun. Netw.*, 2010, pp. 1–16